LONGITUDINAL ACCEPTANCE IN LINEAR NON-SCALING FFAGS*

J. Scott Berg, Brookhaven National Laboratory, P.O. Box 5000, Upton, NY, 11973-5000, USA

Abstract

Linear Non-Scaling FFAGs have, particularly for muon acceleration, a unique type of longitudinal motion. This longitudinal motion can be approximated by a parabolic dependence time-of-flight on energy. This motion can be described in dimensionless variables with two parameters. I describe the relationship between the parameters and the distortion of ellipses in longitudinal space.

INTRODUCTION

Fixed field alternating gradient (FFAG) accelerators are machines which accelerate over a large range of energy (generally a factor of 2 or more) without varying the magnet fields. Since the magnet fields don't vary during acceleration, they allow for very rapid acceleration. A new type of FFAG, the linear non-scaling FFAG [1, 2], has been of interest recently in several applications, particularly for muon acceleration.

For the muon acceleration application in particular, the acceleration must be so rapid that the RF frequency cannot be varied to match the changes in the time of flight with energy. To minimize the rate at which particles get out of phase with the RF, the machine designed to be as isochronous as possible. This leads to a time-of-flight which is nearly parabolic in energy, as shown in Fig. 1.

This paper describes the longitudinal dynamics in a machine where the time of flight is exactly a parabolic function of energy, with the minimum of the parabola at the center of the energy range, and the RF voltage is a sinusoidal function of the phase. In the model, the RF voltage and the time-of-flight advance are both distributed uniformly
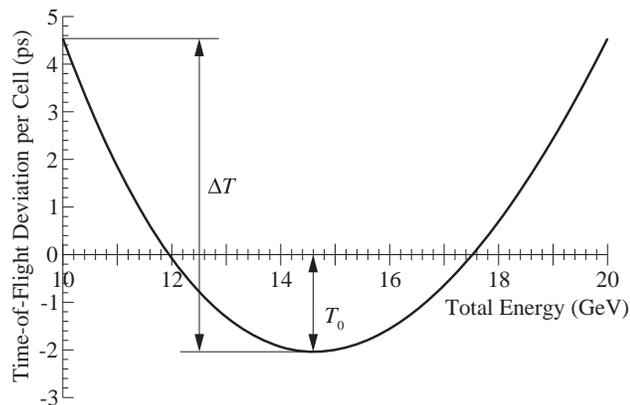

Figure 1: Time of flight as a function of energy.

around the ring. This system has been examined previously [3, 4]. A primary constraint on the design parameters for these FFAGs will be the amount of longitudinal phase distortion one can tolerate. This paper will quantify this distortion and describe a method for computing it for this system.

DESCRIPTION OF DYNAMICS

The equations of motion for our simplified system are

$$\frac{d\tau}{ds} = \Delta T \left(\frac{2E - E_i - E_f}{\Delta E} \right)^2 - T_0 \qquad (1)$$

$$\frac{dE}{ds} = qV \cos(\omega\tau), \qquad (2)$$

where τ is the time-of-flight relative to zero RF phase, s is the distance along a reference curve which defines the coordinate system, E is the particle energy, ΔT and T_0 are as shown in Fig. 1 and are times of flight per unit length along the reference curve, E_i and E_f are the reference energy at injection and extraction respectively, $\Delta E = E_f - E_i$, q is the particle charge, V is the average RF gradient, and ω is the angular RF frequency. I simplify the system further by changing to dimensionless variables

$$x = \omega\tau \qquad p = \frac{E - E_i}{\Delta E} \qquad u = s\omega\Delta T. \quad (3)$$

In these variables, one accelerates from $p = 0$ to $p = 1$. The equations of motion in these variables are

$$\frac{dx}{du} = (2p - 1)^2 - b \qquad \frac{dp}{du} = a \cos x, \qquad (4)$$

where

$$a = \frac{qV}{\omega\Delta T\Delta E} \qquad b = \frac{T_0}{\Delta T}. \qquad (5)$$

These equations of motion arise from a Hamiltonian

$$\frac{1}{6}(2p - 1)^3 - \frac{b}{2}(2p - 1) - a \sin x. \qquad (6)$$

One cannot accelerate from $p = 0$ to $p = 1$ unless

$$\frac{1}{3} - 2a < b < (3a)^{2/3}. \qquad (7)$$

In particular, this requires that $a > 1/24$. Figure 2 shows one example the phase space and a bunch being accelerated in that phase space. Figure 3 shows the region of the a-b parameters space where one can accelerate from $p = 0$ to $p = 1$.
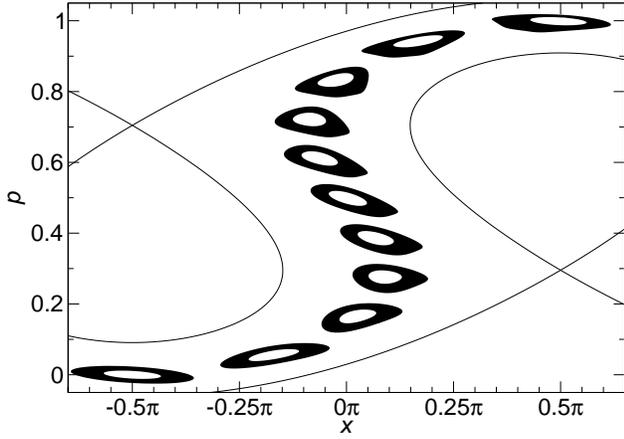
Figure 2: Phase space for the case $a = 1/12$, $b = 1/6$, showing separatrices (solid lines) and a bunch being accelerated from $p = 0$ to $p = 1$.
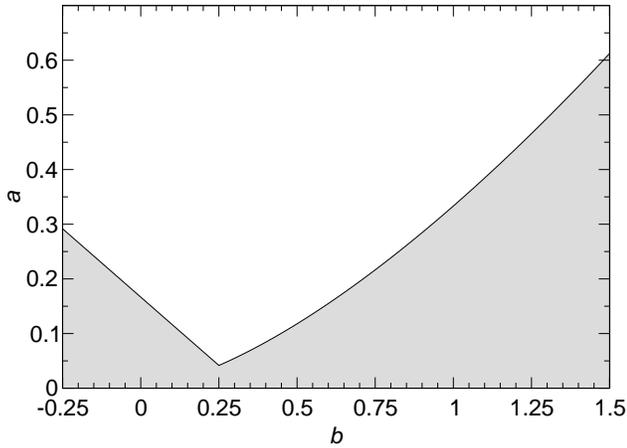

Figure 3: Regions of the a-b parameter space where one can (white) and cannot (grey) accelerate from $p = 0$ to $p = 1$.

COMPUTATION OF DISTORTION

To compute the distortion of the longitudinal phase space, I will use the Dragt-Finn factorization [5]. I will find the map about an orbit that goes through the center of the phase space, $(x, p) = (0, 1/2)$. Due to the symmetries of the problem, this map can be expressed to fifth order as

$$\mathcal{M} = \exp(2{:}e^{-:f_2:}f_3{:}) \exp(2{:}e^{-:f_2:}f_5{:}) \qquad (8)$$

where

$$e^{:f_5:}e^{:f_4:}e^{:f_3:}e^{:f_2:} \qquad (9)$$

is the Dragt-Finn factorization of the map from $(x, p) = (0, 1/2)$ to $p = 1$, which is easily computed as described in [5]. I wish to study the effect of $\mathcal{M}$ on an elliptically symmetric distribution in phase space. If $\mathcal{A} = e^{:a_2:}$ transforms a circularly symmetric distribution into the elliptically symmetric distribution in question, then I can instead

study the effect of

$$\mathcal{M}_C = \exp(2{:}e^{:a_2:}e^{-:f_2:}f_3{:}) \exp(2{:}e^{:a_2:}e^{-:f_2:}f_5{:})$$
$$= e^{:g_3:}e^{:g_5:} \qquad (10)$$

on a circularly symmetric distribution.

The simplest quantity to compute is the emittance, which is the square root of the determinant of the second-order covariance matrix

$$\Sigma(u) = \int \boldsymbol{z}\boldsymbol{z}^T \rho(\boldsymbol{z}, u) d^2\boldsymbol{z}, \qquad (11)$$

where $\rho(\boldsymbol{z}, u)$ is the phase space density at the phase space point $\boldsymbol{z}$ and independent variable u. If one has an initial distribution which is circularly symmetric and has an arbitrary dependence on $J = \boldsymbol{z}^T \boldsymbol{z}/2$ (the usual action variable), then $\mathcal{M}_C$ increases the emittance by

$$\frac{3}{4}\langle J^2 \rangle (9g_{30}^2 + 5g_{31}^2 + 5g_{32}^2 + 9g_{33}^2 - 6g_{30}g_{32} - 6g_{31}g_{33})$$
$$- \frac{1}{2}\langle J \rangle^2 [(g_{31} + 3g_{33})^2 + (g_{32} + 3g_{30})^2], \qquad (12)$$

where

$$g_n = \sum_{k=0}^{n} g_{nk} x^{n-k} p^k. \qquad (13)$$

Note that this can be negative if $\langle J^2 \rangle < 4/3\langle J \rangle^2$ (the phase space density is uniform for equality). For a Gaussian distribution, $\langle J^2 \rangle = 2\langle J \rangle^2$, and in general $\langle J^2 \rangle > \langle J \rangle^2$. This result would hold even if there were a nonzero g_4 in Eq. (10).

At this point we have a procedure for computing the emittance growth for a given a, b, and initial ellipse shape. One generally would like to determine a and b based on the design criteria for the system. Let us assume that the initial ellipse shape can be controlled, and that our only design criterion is that emittance growth is kept to some particular value. In general, b is easily changed in an FFAG, by simply making small changes in the cell length or the RF frequency. However, the choice of a has a major effect on the design of the machine [6, 7]. Thus, the emittance growth will be minimized over the initial ellipse orientation and b. The result is shown in Fig. 4.

The emittance growth is proportional to $\langle J \rangle^2$, as expected and depends strongly on the shape of the distribution. For small a, the emittance growth is proportional to $(a - 1/24)^{-2}$. This is because for small a, the time (in u) to get from $p = 0$ to $p = 1$ is proportional to $-\log(a - 1/24)$, and thus the matrix elements in $e^{:f_2:}$ become proportional to $(a - 1/24)^{-1}$ during the integration, leading to f_3 and g_3 also being proportional to $(a - 1/24)^{-1}$ (see [5]). For a below about 0.4, the minimum b is $1/3 - 2a$.

Since the emittance growth depends strongly on the choice of distribution and can even be negative (an artifact of using the second order covariance matrix), a better performance criterion may be how far an initial ellipse deviates from being an ellipse after applying the
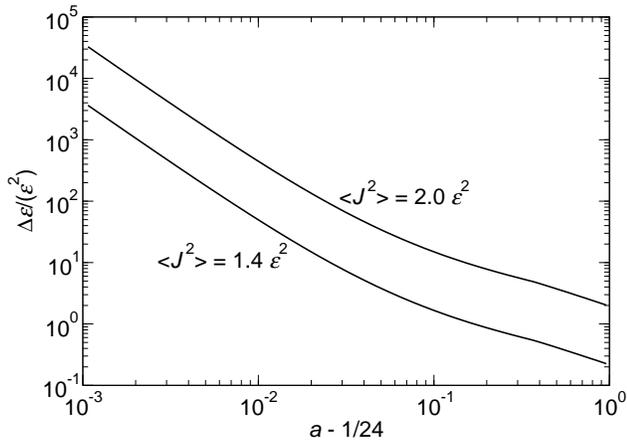
Figure 4: Change in $\varepsilon = \sqrt{\det \Sigma(u)}$ as a function of a.

Figure 5: Relative accuracy of the estimate as a function of the desired $\Delta J/(2J)$, for $a = 0.083$.

map. Starting with the phase-space circle $z_i(J,\theta) = (\sqrt{2J}\cos\theta, \sqrt{2J}\sin\theta)$, one can choose a vector $z_0(J)$ and a symmetric, unit-determinant matrix $B(J)$ so as to minimize

$$\Delta J(J) = \sup_\theta |J_f(J,\theta) - J| \qquad (14)$$

$$J_f(J,\theta) = [z_f(J,\theta) - z_0(J)]^T B(J)[z_f(J,\theta) - z_0(J)], \qquad (15)$$

where $z_f(J,\theta)$ is what $z_i(J,\theta)$ maps to.

If one wants the ellipse center and shape to be independent of J (so that the effective density at the core will not increase from filamentation), z_0 and B will be independent of J. Thus, we find

$$J_f(J,\theta) - J =$$
$$- 2\sqrt{2J^3}[g_{31}\cos^3\theta + (3g_{30} - 2g_{32})\cos^2\theta \sin\theta$$
$$+ (3g_{33} - 2g_{31})\cos\theta \sin^2\theta + g_{32}\sin^3\theta]. \quad (16)$$

Minimizing on the ellipse orientation and b, one obtains curves for $\Delta J/(2J)^{3/2}$ which are similar to those in Fig. 4. For small a, $\Delta J \propto (a-1/24)^{-1}$, for the reasons described above.

If one is only concerned with the outermost ellipse (for instance, if one is not concerned with the core density but only with total transmission), then z_0 and B can be allowed to depend on J. This extra freedom will make ΔJ proportional to $(2J)^{5/2}$ and $(a - 1/24)^{-3}$ for small a, with the curve for $\Delta J/(2J)^{5/2}$ again being qualitatively similar to those in Fig. 4. If there were g_4 terms in Eq. (10), the solution would still be the same in the $a \to 1/24$ limit, but the g_4 terms could potentially dominate for larger a. However, the symmetry breaking is expected to be small (see Fig. 1 for a real example), so this computation in general will give a good estimate.

Figure 5 shows one example of the accuracy of this computation as a function of the desired accuracy. To produce the plot, I chose a given a, computed the ellipse distortion allowing J dependence in z_0 and B, computed what
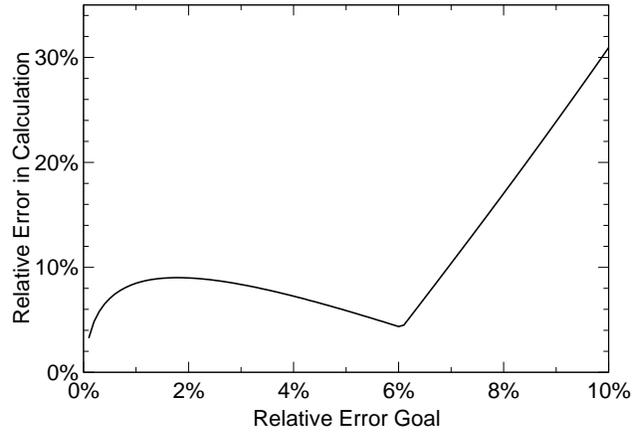
J corresponds to a given $\Delta J/(2J)$, and tracked particles on the optimal ellipse with that J. One sees that the estimate is good for small $\Delta J/(2J)$, but quickly gets worse once $\Delta J/(2J)$ gets sufficiently large. The ellipse gets so distorted for large amplitudes that the power series representation cannot give a good approximation to its shape.

REFERENCES

[1] C. Johnstone, W. Wan, and A. Garren, "Fixed Field Circular Accelerator Designs," in *Proceedings of the 1999 Particle Accelerator Conference, New York, 1999*, A. Luccio and W. MacKay, eds. (IEEE, Piscataway, NJ, 1999) p. 3068.

[2] F. E. Mills and C. Johnstone, in the transparency book for the 4th International Conference on Physics Potential & Development of $\mu^+ \mu^-$ colliders, San Francisco, CA (UCLA, Los Angeles, 1997), pp. 693–698.

[3] J. Scott Berg, "Dynamics in Imperfectly-Isochronous FFAG Accelerators," in *Proceedings of EPAC02, Paris France*, (EPAC, European Physical Society Accelerator Group, 2002) p. 1124.

[4] S. Koscielniak and C. Johnstone, "Longitudinal Dynamics in an FFAG Accelerator Under Conditions of Rapid Acceleration and Fixed, High RF," in *Proceedings of the 2003 Particle Accelerator Conference*, Joe Chew, Peter Lucas, and Sara Webber, eds. (IEEE, Piscataway, NJ, 2003).

[5] Alex J. Dragt and Étienne Forest, "Computation of nonlinear behavior of Hamiltonian systems using Lie algebraic methods," J. Math. Phys. **24** (1983), p. 2734.

[6] J. Scott Berg and Robert B. Palmer, "Cost Optimization of Non-Scaling FFAG Lattices for Muon Acceleration," in *Proceedings of EPAC 2004, Lucern, Switzerland*, (EPAC, European Physical Society Accelerator Group, 2004) p. 587.

[7] J. Scott Berg, "Recent Results from Optimization Studies of Linear Non-Scaling FFAGs for Muon Acceleration," to appear in the proceedings of FFAG 04, KEK, Tsukuba, Japan, 13–16 October 2004. Preprint MUC-CONF-ACCELERATION-309, available from http://www-mucool.fnal.gov/notes/notes.html.